

IMECE2020-23816

NUMERICAL SIMULATION OF STRESS STATES IN WHITE MATTER VIA A CONTINUUM MODEL OF 3D AXONS TETHERED TO GLIA

Parameshwaran Pasupathy¹, Robert De Simone², Assimina A Pelegri^{1*}

¹Department of Mechanical and Aerospace Engineering
Rutgers, The State University of New Jersey, Piscataway, NJ.

²Marotta Controls, Inc, 78 Boonton Avenue, Montville, NJ.

ABSTRACT

A new finite element approach is proposed to study the propagation of stress in axons in the central nervous system (CNS) white matter. The axons are embedded in an extra cellular matrix (ECM) and are subjected to tensile loads under purely non-affine kinematic boundary conditions. The axons and the ECM are described by the Ogden hyperelastic material model. The effect of tethering of the axons by oligodendrocytes is investigated using the finite element model. Glial cells are often thought of as the “glue” that hold the axons together. More specifically, oligodendrocytes bond multiple axons to each other and create a myelin sheath that insulates and supports axons in the brainstem. The glial cells create a scaffold that supports the axons and can potentially bind 80 axons to a single oligodendrocyte.

In this study, the microstructure of the oligodendrocyte connections to axons is modeled using a spring-dashpot approximation. The model allows for the oligodendrocytes to wrap around the outer diameter of the axons at various locations, parameterizing the number of connections, distance between connection points, and the stiffness of the connection hubs. The parameterization followed the distribution of axon-oligodendrocyte connections provided by literature data in which the values were acquired through microtome of CNS white matter. We develop two models: 1) multiple oligodendrocytes arbitrarily tethered to the nearest axons, and 2) a single oligodendrocyte tethered to all the axons at various locations. The results depict stiffening of the axons, which indicates that the oligodendrocytes do aid in the redistribution of stress. We also observe the

appearance of bending stresses at inflections points along the tortuous path of the axons when subjected to tensile loading. The bending stresses appear to exhibit a cyclic variation along the length of the undulated axons. This makes the axons more susceptible to damage accumulation and fatigue. Finally, the effect of multiple axon-myelin connections in the central nervous system and the effect of the distribution of these connections in the brain tissue is further investigated at present.

Keywords: micromechanics, multi-scale modeling, hyperelastic, finite element, Abaqus, oligodendrocyte, axonal injury, brain, CNS white matter.

1 INTRODUCTION

Traumatic Brain Injury (TBI) is one of the most researched topics of the 21st century. In recent years, the number of TBI diagnoses have increased rapidly. However, efforts to accurately measure and predict cerebral injury have been a major challenge. The corpus callosum has been identified as a critical region for TBI with axonal injury being the proximal cause [1]. Axonal damage has been identified as the leading cause of TBI, with excessive tensile strain postulated as the underlying mechanism [1]. The use of finite element methods to predict and understand axonal injury have nevertheless yielded significant breakthroughs. An inverse finite element (FE) method to predict material properties of the axons by matching experimental data with simulations was first proposed by Pan et al [2-4]. Yousefsani et al developed an FE model using the embedded element technique to bind axons

*Contact author: pelegri@rutgers.edu

of varying diameters to the ECM when subjected to transverse loading [5]. Karami et al used a fiber reinforced composite model to represent an axon following a sinusoidal path embedded in the ECM and subject to bending, tension and shear [6]. All of the above studies use affine boundary conditions which tie the axon entirely to the ECM. In reality, the axons do not exhibit a purely affine behavior. They display a “transitional” behavior from non-affine behavior at low stretch to affine behavior at high stretch values when tortuosity decreases [4].

Oligodendrocytes are specialized glial cells that wrap around the axons via a sheath of myelin. The mechanical response of myelinated axons was first investigated by Shreiber et al [7-8]. The results show that myelination improves the stiffness of the axons. The effect of tethering by the oligodendrocyte “arms” however, is not well documented. In this study, a proof of concept model has been developed to probe the effect of the tethering by the oligodendrocytes. The model also incorporates a purely non-affine boundary condition between the axons and the ECM. The methods employed and the results obtained are presented here.

2 MATERIALS AND METHODS

2.1 MICROMECHANICAL FINITE ELEMENT MODEL

The microscale FE models have been developed using Abaqus 6.14-2 and Python scripting. The representative volume element of the axons tethered to glia in CNS white matter is based on the models developed by Pan et al [2]. Axons of varying undulation and radii are embedded in a 3-D rectangular ECM of dimensions: $x = 0.9 \mu m$, $y = 8 \mu m$, $z = 5.747 \mu m$. The undulation is different from axon to axon and is based on the work by Bain et al [9]. The average undulation varies from 1.00 to 1.10. The diameter of the axons varies between a minimum of $0.4 \mu m$ to a maximum of $0.62 \mu m$ with an average axon diameter of $0.45 \mu m$. Using symmetry boundary conditions in x and y , one half of the model is used for the analysis. The volume fraction of the axons is 50 percent. A total of 9 axons are lodged within the ECM. Non-affine boundary conditions between the axons and ECM are established using a “surface to surface” contact definition as shown in Figure 1. The surface constitutive model for contact used in Abaqus defines the contact pressure between surfaces of axon and ECM, p as a function of the “overclosure,” h , of the surfaces such that: $p = 0$ for $h < 0$ and $p > 0$ for $h = 0$ [10].

Oligodendrocytes have long been known to produce myelin which wraps around the axon. The myelin electrically insulates the axon and also mechanically tethers the axon to adjacent ones. Oligodendrocytes have been recorded to bond up to 80 separate axons. Myelinated axons demonstrate a much higher stiffness in response to tensile loads in comparison to demyelinated axons. This demonstrates that the glial cells provide significant mechanical support to the axons and dictates the response of the

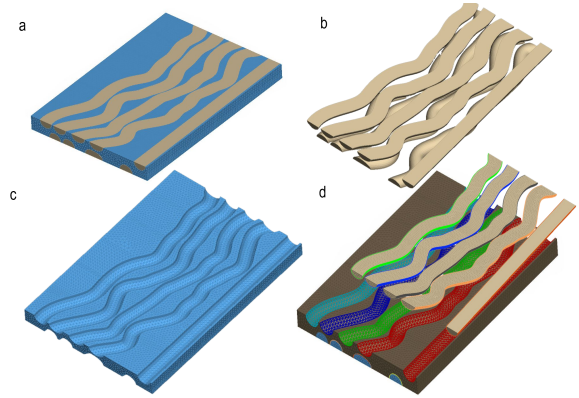


FIGURE 1. a) FE Model of the ECM and Axon assembly b) FE model depicting the undulation of the Axons c) FE model of ECM d) Contact surfaces defining surface to surface contact between Axon and ECM.

axons to tensile loads [7-9]. While the impact of myelination on the stiffness of the axons has been well documented [9-10], the effect of tethering of the oligodendrocyte and its impact on the mechanical response of the axons is not well understood.

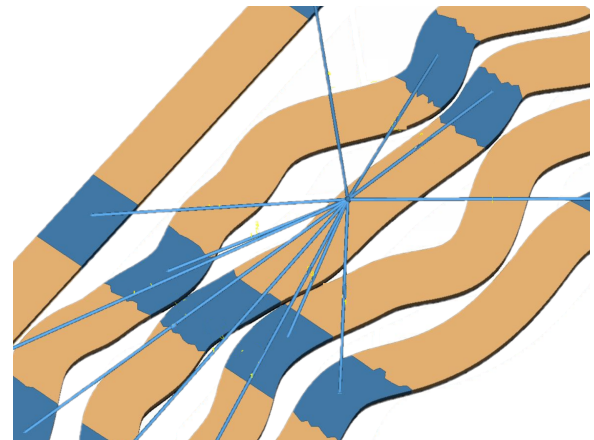


FIGURE 2. A schematic representation of an oligodendrocyte tethering to axons at different locations via a sheath of myelin.

In this study, a method to probe the effect of tethering of oligodendrocytes on the mechanical response of axons is explored. We posit a spring-dashpot approximation to model the arms of the oligodendrocyte that tether to the axons. The scope of the study is limited to characterizing the mechanical response of the arms of the oligodendrocyte and not the nucleus itself. Therefore, the nucleus is modeled as a distributed coupling constraint in Abaqus. A distributed coupling constrains the motion of a group of nodes called the “coupling nodes” to the translation and rotation of the reference node. The constraint allows for the distribution

of loads through a weighting factor between the reference and the coupling nodes based on a user specified influence radius. Here, the oligodendrocyte is visualized as a sphere of $0.025 \mu\text{m}$ embedded inside the ECM. The reference node of the distributed coupling is located at the center of the sphere. The nodes of the ECM along the surface of the sphere are the coupling nodes. The influence radius is set to the radius of the sphere with a uniform weighting method and a weight factor of 1. In order to allow the oligodendrocyte to wrap around the axon, each axon is sliced into several sections. The nodes along the surface of each section is tied to a remote point at the center of the section using a coupling constraint. A linear spring-dashpot connects the remote point on the axon to the center of the oligodendrocyte sphere as shown in Figure 3.

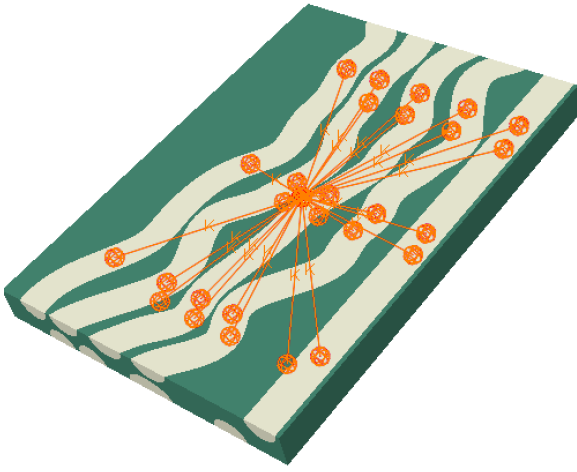


FIGURE 3. FE Model of oligodendrocyte tethering to axons embedded in ECM.

2.2 HYPERELASTIC MATERIAL MODEL

Nonlinear hyperelastic models are often used for the simulation of soft biological tissues. Meaney [11] developed a mathematical relationship between microstructurally based models of the central nervous system (CNS) white matter and equivalent hyperelastic material models. Pan et al [2-4] used the Ogden hyperelastic material model for the simulation of kinematics of CNS white matter and in their optimization procedure to identify material properties using an inverse FE method. Karami et al [6] used the Ogden hyperelastic model in their fiber reinforced composite model of CNS white matter. Yousefsani et al [5] used the Ogden hyperelastic model in developing the embedded element technique for brain white matter. Mihai et al [12] developed a family of hyperelastic modeling approaches using experimental results from multiaxial loading of brain samples.

In this study, we used the Ogden hyperelastic material model to simulate the ECM and the axons. The versatility of the Ogden model allows for neural tissue to be characterized relatively easily. The Ogden hyperelastic model is based on the three principal stretches $\lambda_1, \lambda_2, \lambda_3$ and $2N$ material constants. The strain energy density function, W , for the Ogden material model in Abaqus is formulated as [10]:

$$W = \sum_1^N \frac{2\mu_i}{\alpha_i^2} (\bar{\lambda}_1^{\alpha_i} + \bar{\lambda}_2^{\alpha_i} + \bar{\lambda}_3^{\alpha_i} - 3) + \sum_1^N \frac{1}{D_i} (J_{el} - 1)^{2i} \quad (1)$$

where $\bar{\lambda}_i = J^{-\frac{1}{3}} \lambda_i$ and $\bar{\lambda}_1 \bar{\lambda}_2 \bar{\lambda}_3 = 1$. μ_i are shear moduli, α_i and D_i are material parameters. The first and the second terms represent the deviatoric and hydrostatic components of the strain energy function. The parameter $D_1 = \frac{2}{K_0}$, allows for the inclusion of compressibility where K_0 is the initial bulk modulus. An incompressible, single parameter Ogden hyperelastic material is considered in this study. Therefore, $N = 1$. Incompressibility implies that $J_{el} = 1$ and is specified in Abaqus by setting $D_1 = 0$. As a result, Abaqus eliminates the hydrostatic component of the strain energy density equation, and the expression reduces to the following:

$$W = \sum_1^N \frac{2\mu_i}{\alpha_i^2} (\lambda_1^{\alpha_i} + \lambda_2^{\alpha_i} + \lambda_3^{\alpha_i} - 3). \quad (2)$$

For uniaxial tension, the principal stress is given by:

$$\sigma_{uniaxial} = \frac{2\mu}{\alpha} \left[\lambda^\alpha - \left(\frac{1}{\sqrt{\lambda}} \right)^\alpha \right] \quad (3)$$

Undulation prevents the axons from experiencing full tension until a threshold strain is reached and the undulation for the axon becomes 1. The values for the shear modulus for the axons and ECM are based on research by Wu et al [13]. The value of α is based on the model developed by Meaney [11]. The shear modulus of the ECM is assigned based on the shear modulus of the axon, as the axon is three times stiffer than the ECM as reported by Arbogast and Marguile's findings [1]. To model incompressibility of the hyperelastic materials, we use a special family of hybrid elements available in Abaqus. In an incompressible material, a tiny change in displacement can produce an extremely large change in pressure. As a result, a purely displacement-based solution is too sensitive to achieve meaningful solutions. Abaqus treats this singular behavior by interpolating the hydrostatic pressure independently as a basic

Material Properties				
Component	μ (MPa) [13]	D (1/MPa)	$\alpha[11]$	Element Type
Axon	$2.150 \cdot 10^{-3}$	0	6.19	C3D8H, C3D4H
ECM	$0.850 \cdot 10^{-3}$	0	6.19	C3D4H

TABLE 1. Material Properties for the FE Model



FIGURE 4. Submodel-1: Oligodendrocytes arbitrarily tethered to axons

solution variable coupled to the displacement solution through the constitutive theory and compatibility conditions [10]. The modified Cauchy stress is therefore written by introducing an independent hydrostatic pressure field \hat{p} as [8]:

$$\bar{\sigma} = \sigma + (1 - \rho)\mathbf{I}(p - \hat{p}), \quad (4)$$

where p is the hydrostatic stress component and ρ is a small number. This modified expression for the Cauchy stress is used in the expression for virtual work with a Lagrange multiplier enforced constraint $\Delta p - \Delta \hat{p} = 0$. Table 1 shows the material properties and the element types used in the FE model.

2.3 FINITE ELEMENT SUBMODELS

To study the effect of tethering of oligodendrocyte on the mechanical response of axons, two submodels have been developed. For the first submodel, a plane between the axon layers is created and 25 grid points are evenly spaced. The oligodendrocyte nucleus is generated as a sphere with a radius of $0.025 \mu\text{m}$ at each point. The oligodendrocyte spheres are attached to any axon connection point that lay within a radius of $0.05 \mu\text{m}$ by a spring-dashpot connection. The maximum number of axons connected to a single oligodendrocyte is 4, with some oligodendrocytes only connecting to one axon (Figure 4).

For the second submodel, a single oligodendrocyte is tied to all the axons at different locations. The oligodendrocyte is placed at the center of the ECM. The number of connections between the axons and the oligodendrocyte is parameterized as shown in Figure 5. As detailed in previous sections, spring-dashpot elements simulate the tethering arms of the oligodendrocyte. An exhaustive literature search yielded no studies or test data that characterize the stiffness of the oligodendrocytes. Therefore, in this study, the stress-strain response of the axons were obtained by parameterizing the stiffness of the spring-dashpot connection. Since oligodendrocytes essentially tether to the axons via a sheath of myelin, the material properties of myelin served as the upper limit for the parameterization of the oligodendrocyte stiffness.

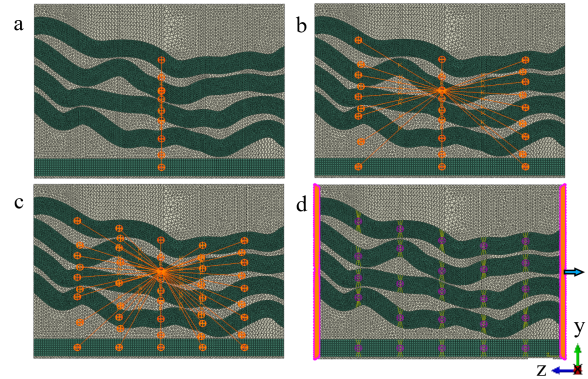


FIGURE 5. a-c) Parameterization of number of connections between oligodendrocyte and each axon in submodel-2 - Showing 1,3 and 5 connections per axon d) boundary conditions for the FE model with the left end fixed and a stretch applied on the right.

The FE model is set up with symmetry boundary conditions on the top and bottom faces in x coordinate direction and side faces in y coordinate direction. The model is constrained in the z direction using fixed boundary conditions on one face and a stretch applied to the opposite face using a non-zero displacement boundary condition. An implicit time integration technique in Abaqus is used to solve the FE model. Contact stabilization is used to prevent rigid body modes before contact is established between the interacting surfaces of the axons and ECM.

3 RESULTS AND DISCUSSION

A Von Mises stress plot for the axons and the ECM subjected to 20 percent stretch in z direction is shown in Figure 6. Undulation prevents the axons from experiencing full tension. The undulation and the interaction of the axons with the ECM creates high stress in the concave regions. High stress would occur in

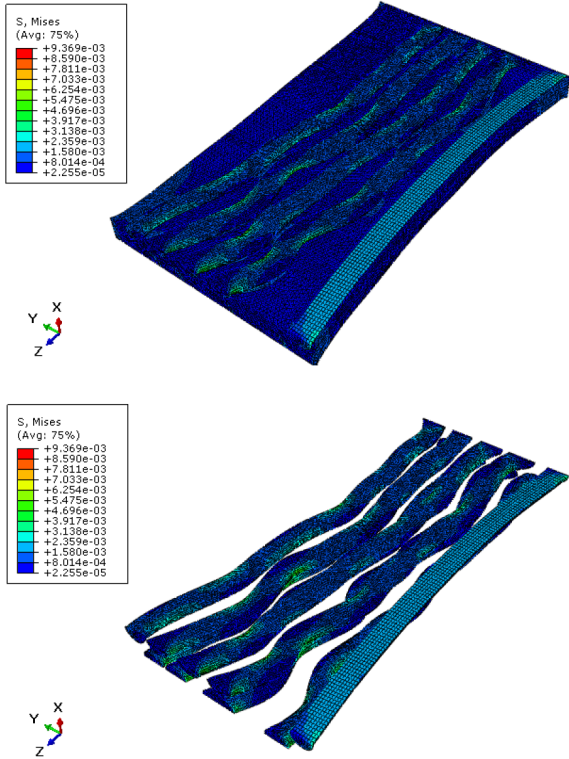


FIGURE 6. Von Mises stress contour for the Axons and the ECM at 20 percent applied stretch. Undulation of axons result in high stress in the concave regions.

these regions even if the axons are subjected to purely affine boundary conditions. However, allowing the axons to interact with the ECM through non-affine boundary conditions creates a more even stress distribution in both the axons and the ECM. It can be seen in Figure 6 that the straight axon (with undulation = 1) is in full tension. The undulated axons however experience bending stresses along their tortuous path. These bending stresses appear to undergo cyclic reversal from tension to compression at each inflection point along the length of axon as seen in Figure 7. This makes the axons more susceptible to damage accumulation and failure due to fatigue. Traumatic events such as large and sudden impacts are known to cause diffuse axonal injury (DAI), but the mechanics behind cumulative damage is still unknown. Further research is essential to understand the susceptibility of axons to fatigue failure.

A comparison of the stress-strain response for submodel-1 and submodel-2 with the oligodendrocyte arm stiffness set to $10 N/m$ is shown in Figure 8. Submodel-1 contains a total of 25 oligodendrocyte spheres tethering to the nearest axons while submodel-2 contains a single oligodendrocyte at the FE model center tethered to all the axons. Here, submodel-2 has 5 oligodendrocyte connections per axon. It is observed that the

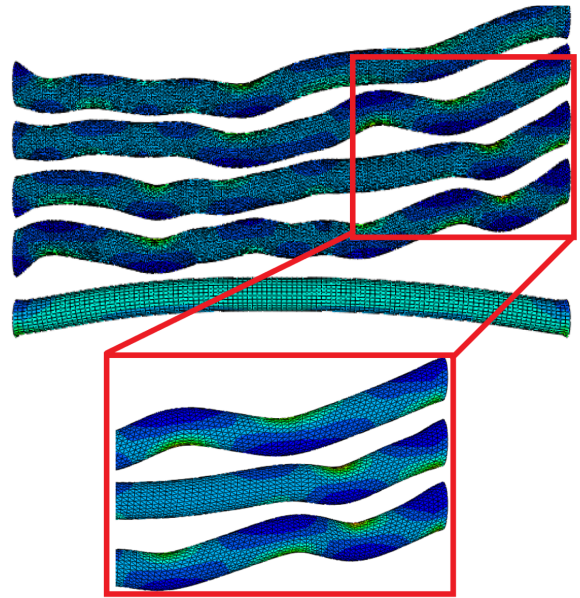


FIGURE 7. Bending stresses undergoing full reversal from tension to compression.

response of the two models are nearly identical with submodel-1 indicating a slightly higher stiffness in response to tensile loads. The root mean square deviation (RMSD) between the two curves is 0.00139, where RMSD is defined as $\sqrt{\frac{\sum (f(x_i) - g(x_i))^2}{N}}$ for curves $f(x)$, $g(x)$ and N being the number of points x_i at which the curves are compared. Looking at Figure 9, which compares the stress-strain response for submodel-2 with different number of oligodendrocyte connections per axon, it is observed that the responses are again nearly identical. Upon closer inspection, it is seen that the difference in stress-strain response between 3 and 5 connections per axon is much smaller with RMSD 0.00131 than the difference between 1 and 3 connections per axon with RMSD 0.00341. Thus, it is noted that there is only a modest increase in the stiffness of the axons with increasing number of oligodendrocyte connections per axon.

From Figures 8,9 it can also be inferred that for nearly the same number of total oligodendrocyte connections per axon, the stress response is almost identical. The response is independent of whether the number of connections come from a single oligodendrocyte or if they come from multiple oligodendrocytes. This explains the near identical behavior of submodels 1,2. The FE model is subjected to a maximum applied stretch of up to a 100 percent. For an applied stretch of 90 percent and above, the axons in the FE model containing a single oligodendrocyte connection reach an undulation of 1 and begin to experience full tension. This can be observed in the increased stiffening response of the “1 connection per axon” model shown in figure 9.

As mentioned in the previous section, this study is limited

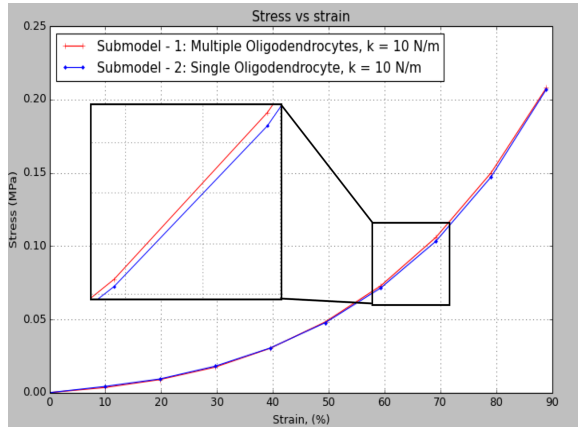


FIGURE 8. Stress-strain response for submodels 1, 2. The stiffness of the oligodendrocyte is set to 10 N/m. For this comparison, submodel 2 has 5 oligodendrocyte connections per axon.

to characterizing the impact on the stiffening of the axons due to tethering by the oligodendrocyte connections and not the oligodendrocyte itself. The stiffening response of the axons due to oligodendrocytes is in general agreement with the trends observed by Pan et al [4]. The transitional behavior from non-affine to affine boundary conditions as described by Pan et al is due to a larger recruitment of nodes of Ranvier as the axons stretch thus causing the axons to stiffen [4]. Similarly, each connection between an oligodendrocyte and the axon results in the creation of a node of Ranvier. An increasing number of connections imply a greater number of nodes being created and thus, a stiffer axon. The creation of these nodes are independent of if the connections are made with a single oligodendrocyte or with multiple oligodendrocytes as seen in the comparison between submodels 1 and 2 (Figure 8).

Finally, the results for the response of submodel-2 for different stiffness values of the oligodendrocyte arms is shown in Figure 10. The FE model with 5 oligodendrocyte connections per axon is subjected to increasing strains up to a maximum of a 100 percent applied stretch. The response is recorded for different spring-dashpot stiffness values. It is observed that the model becomes increasingly stiffer with higher values of “k”. This indicates that the oligodendrocytes do act as a supporting scaffold for the axons in addition to the stiffening provided by the myelin sheath.

4 CONCLUSIONS

In this study, a 3-D simulation of two submodels of axons embedded in an ECM have been developed to understand the mechanical response of axons tethered to the oligodendrocytes using purely non-affine boundary conditions. Undulated axons embedded in the ECM experience bending stresses that appear

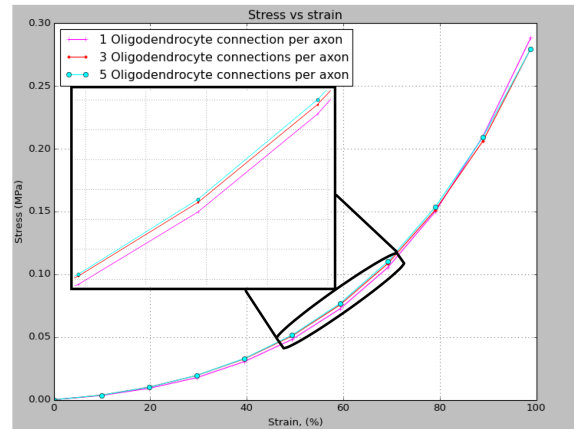


FIGURE 9. Stress-strain response for submodel-2 parameterizing the number of connections between the oligodendrocyte and the axons.

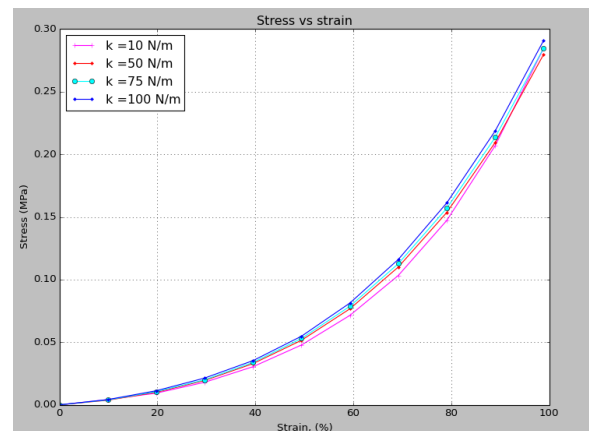


FIGURE 10. Stress-strain response for submodel-2 parameterizing the stiffness of the oligodendrocyte arms. Simulations performed for 5 oligodendrocyte connections per axon.

to undergo cyclic reversal along their tortuous paths. This makes the axons susceptible to failure due to fatigue. Traumatic events such as DAI will destroy axons over a very short period (within milliseconds), while repeated stresses can take anywhere from tens to millions of cycles before failure. Like ductile materials, hyperelastic materials also suffer from low and high cycle fatigue [14]. The magnitude of the bending stress will largely depend on the geometry of the axons – which is mostly random. Differences in brain mass and load direction for each individual axon will also play a large part in damaging the cerebral region [15]. Future work incorporating damage models for the axons subjected to cyclic loads is essential to understand axonal fatigue and trauma due to damage accumulation from repeated impact to the brain.

Parameterization of number of oligodendrocyte connections per axon reveal that the axons exhibit increased stiffness for

increasing number of connections. However, it is immaterial if the total number of connections are provided by a single oligodendrocyte or multiple oligodendrocytes. This is in agreement with the trends observed by Pan et al [4]. The increase in the number of connections between an axon and the oligodendrocyte results in a larger recruitment of nodes of Ranvier, which aids the stiffening response of the axons. Creation of nodes of Ranvier is independent of if the connections are made with a single or multiple oligodendrocytes. Parameterization of the stiffness of the oligodendrocyte connections also reveal that the axons exhibit a stiffer behavior to tensile load for oligodendrocyte arms with greater stiffness. This indicates that the oligodendrocyte connections do aid in the mechanical response of the axons to external loading. While it is well established that oligodendrocytes support the axons by creating a sheath of myelin around the axons, this study, in addition, also suggests the possibility of a direct influence on the mechanical response of the axons due to the act of tethering by the oligodendrocytes.

This study has potential limitations. As described in the introduction, axons exhibit a transitional behavior from non-affine boundary conditions at low stretch to a purely affine behavior at higher stretches. This study approximates a non-affine boundary condition for the entire stretch history. Future models that incorporate this transition mechanism from non-affine to affine behavior as a function of tortuosity will yield more accurate results. The study also approximates the oligodendrocyte connections using a linear spring-dashpot connections. Finally, this model does not incorporate damage initiation and evolution. Bending stresses that undergo cyclic reversal are prominent in the undulated axons. A 3-D model that incorporates damage accumulation and fatigue analysis will yield a more comprehensive picture of the structural response of axons to external loading.

5 REFERENCES

- [1] Arbogast KB, Margulies SS. "Material characterization of the brainstem from oscillatory shear tests." *Journal of Biomechanics*. Vol. 31, No. 9 (1998): pp 801–807. DOI 10.1016/s0021-9290(98)00068-2
- [2] Pan Y, Sullivan D, Shreiber DI, Pelegri AA. "Finite Element Modeling of CNS White Matter Kinematics: Use of a 3D RVE to Determine Material Properties." *Front Bioeng Biotechnol*. Vol. 1 (2013): pp 1-19. DOI 10.3389/fbioe.2013.00019
- [3] Singh S, Pelegri AA, Shreiber, D. "Characterization of the three-dimensional kinematic behavior of axons in central nervous system white matter." *Biomech Model Mechanobiol*. Vol. 14 (2015): pp 1303–1315. DOI 10.1007/s10237-015-0675-z
- [4] Pan Y, Shreiber DI, Pelegri AA. "A Transition Model for Finite Element Simulation of Kinematics of Central Nervous System White Matter." *IEEE Transactions on Biomedical Engineering*. Vol. 58, No. 12 (2011): pp 3443-3446, DOI 10.1109/TBME.2011.2163189
- [5] Yousefsani SA, Shamloo A, Farahmand F. "Micromechanics of brain white matter tissue: A fiber-reinforced hyperelastic model using embedded element technique." *Journal Mech Behav Biomed Mater*. Vol. 80 (2018): pp 194-202. DOI 10.1016/j.jmbbm.2018.02.002
- [6] Karami G, Grundman N, Abolfathi N, Naik A, Ziejewski M. "A micromechanical hyperelastic modeling of brain white matter under large deformation." *Journal of the Mechanical Behavior of Biomedical Materials*. Vol. 2, No. 3 (2009): pp 243-254. DOI 10.1016/j.jmbbm.2008.08.003
- [7] Hao H, Shreiber DI. "Axon kinematics change during growth and development." *Journal of Biomech Eng*. Vol. 129, No. 4 (2007): pp 511-522. DOI 10.1115/1.2746372
- [8] Shreiber DI, Hao H, Elias RA. "Probing the influence of myelin and glia on the tensile properties of the spinal cord." *Biomech Model Mechanobiol*. Vol. 8(2009): pp 311-321. DOI 10.1007/s10237-008-0137-y
- [9] Bain AC, Meaney D. "Tissue-level thresholds for axonal damage in an experimental model of central nervous system white matter injury." *Journal of Biomech Eng*. Vol. 122, No. 6 (2000): pp 615–622. DOI 10.1115/1.1324667
- [10] ABAQUS, ABAQUS Theory Manual, Hibbitt, Karlsson and Sorensen Inc, Pautucket, RI, USA (1994)
- [11] Meaney D. "Relationship between structural modeling and hyperelastic material behavior: application to CNS white matter." *Biomechan Model Mechanobiol*. Vol. 1(2003): pp 279-293. DOI 10.1007/s10237-002-0020-1
- [12] Mihai LA, Budday S, Holzapfel GA, Kuhl E, Goriely A. "A family of hyperelastic models for human brain tissue." *Journal of the Mechanics and Physics of Solids*. Vol. 106 (2017): pp 60-79. DOI 10.1016/j.jmps.2017.05.015
- [13] Wu X, Georgiadis JG, Pelegri AA. "Brain White Matter Model of Orthotropic Viscoelastic Properties in Frequency Domain." *Proceedings of the ASME 2019 International Mechanical Engineering Congress and Exposition*. Vol. 3: Biomedical and Biotechnology Engineering. Salt Lake City, Utah, USA (2019) V003T04A024. DOI 10.1115/IMECE2019-12182
- [14] Ayoub G, Zaïri F, Naït-Abdelaziz M, Gloaguen JM. "Modeling the low-cycle fatigue behavior of visco-hyperelastic elastomeric materials using a new network alteration theory: Application to styrene-butadiene rubber." *Journal of the Mechanics and Physics of Solids*. Vol. 59, No. 2 (2011): pp 473–495. DOI 10.1016/j.jmps.2010.09.016
- [15] Kleiven S. "Evaluation of head injury criteria using a finite element model validated against experiments on localized brain motion, intracerebral acceleration, and intracranial pressure." *International Journal of Crashworthiness*. Vol. 11, No. 1 (2006): pp 65–79. DOI 10.1533/ijcr.2005.0384